2016

Investigation of spin-gapless semiconductivity and half-metallicity in Ti_2MnAl-based compounds

Pavel V. Lukashev
University of Nothern Iowa, pavel.lukashev@uni.edu

Parashu Kharel
South Dakota State University, University of Nebraska-Lincoln, pkharel2@unl.edu

S. Gilbert
South Dakota State University, Brookings

B Staten
University of Nothern Iowa

N. Hurley
University of Northern Iowa

See next page for additional authors

Investigation of spin-gapless semiconductivity and half-metallicity in Ti_2MnAl-based compounds

P. Lukashev,[1,a)] P. Kharel,[2,3,b)] S. Gilbert,[2] B. Staten,[1] N. Hurley,[1] R. Fuglsby,[2] Y. Huh,[2] S. Valloppilly,[3] W. Zhang,[3,4] K. Yang,[2,5] R. Skomski,[3,4] and D. J. Sellmyer[3,4]
[1]*Department of Physics, University of Northern Iowa, Cedar Falls, Iowa 50614, USA*
[2]*Department of Physics, South Dakota State University, Brookings, South Dakota 57007, USA*
[3]*Nebraska Center for Materials and Nanoscience, University of Nebraska, Lincoln, Nebraska 68588, USA*
[4]*Department of Physics and Astronomy, University of Nebraska, Lincoln, Nebraska 68588, USA*
[5]*College of Mechanical and Electrical Engineering, Hohai University, Changzhou, Jiangsu 213022, China*

(Received 29 February 2016; accepted 25 March 2016; published online 4 April 2016)

The increasing interest in spin-based electronics has led to a vigorous search for new materials that can provide a high degree of spin polarization in electron transport. An ideal candidate would act as an insulator for one spin channel and a conductor or semiconductor for the opposite spin channel, corresponding to the respective cases of half-metallicity and spin-gapless semiconductivity. Our first-principle electronic-structure calculations indicate that the metallic Heusler compound Ti_2MnAl becomes half-metallic and spin-gapless semiconducting if half of the Al atoms are replaced by Sn and In, respectively. These electronic structures are associated with structural transitions from the regular cubic Heusler structure to the inverted cubic Heusler structure. [http://dx.doi.org/10.1063/1.4945600]

Recently, an interesting new class of materials, namely, spin-gapless semiconductors, has attracted much attention due to potential applications in spintronics.[1–6] These materials are characterized by a zero band gap in one spin channel and by a finite band gap in the other channel, and therefore are different from ferromagnetic materials with semiconducting electron transport, including dilute magnetic semiconductors, which have long been investigated for semiconductor spintronics.[7,8] Spin-gapless semiconductors (SGS) are attractive because they combine advantages of half-metallic (HM) magnets and zero-gap semiconductors. This unique combination leads to several remarkable properties such as high spin polarization (100%) of both the electrons and holes, carrier mobilities much higher than those of classical semiconductors, voltage-tunable spin polarization, and the ability to switch between spin-polarized *n*- and *p*-type conduction.[1,9]

There are several examples of gapless semiconductors, such as graphene and some mercury-based compounds, such as HgCdTe, HgCdSe, and HgZnSe,[10,11] but *spin*-gapless semiconductors pose a much bigger challenge. A few materials, such as Heusler-type Mn_2CoAl and CoFeCrAl, have been realized experimentally,[4,5] but a large part of the current research focuses on predicting SGS theoretically. In 2008, Wang suggested an approach to design SGS materials by doping gapless semiconductors (GS) with magnetic ions, for example, replacing 25% of Pd in $PbPdO_2$ with Co.[1] Since then, more materials, especially derived from Heusler compounds, have been predicted to be SGSs.[2,12]

A specific aim of SGS research is to develop materials having compensated ferrimagnetic or antiferromagnetic spin structures, such as half-metallic antiferromagnets (HM-AFMs).[3,12,13] Compared to ferromagnetic SGSs, these materials exhibit either small or no net magnetization, which is favorable due to the absence of magnetic stray fields, which could otherwise cause interference between neighboring elements in nanoelectronic devices.

The unique band-gap structure of SGSs requires well-defined atomic arrangements and has very narrow margins as far as chemical substitutions and disorder are concerned. The reason is that such structural changes modify the local densities of states (DOS)[4] and amount to a smearing of the total density of states, to a finite resistivity at zero temperature, and to a "dirty-metal" contribution to the transport behavior. In this paper, we investigate the previously unconsidered and probably rare situation in which a partial chemical substitution actually *creates* an SGS. The system is substituted Ti_2MnAl, where half of the Al atoms are replaced by elements such as In and Sn. The parent alloy, Ti_2MnAl, is a bcc (A2) derivative predicted to crystallize in the regular cubic Heusler structure ("regular phase," prototype Cu_2MnAl) while having an inverted cubic Heusler polymorph ("inverted phase," prototype $CuHg_2Ti$) with a slightly higher energy and a SGS band structure with zero net magnetic moment.[3,13,14]

Figure 1 shows the main crystal structures involved in the present paper. The regular cubic Heusler structure (a) and the inverted cubic Heusler structure (b) have 16 atoms per unit cell, and these supercells can be considered as $2 \times 2 \times 2$ superlattices composed of CsCl (c) or bcc (d) unit cells with two atoms each. Both the regular and inverted structures have one Ti atom at the corners of the supercell and three Ti atoms in the middle of the faces of the supercell (Wyckhoff positions 4a). These Ti atoms will be referred to as Ti-1 below. The difference between the regular and inverted structures is best rationalized by the occupancy of the remaining Ti atoms, which we call Ti-2 below. In the regular structure, these Ti atoms occupy the 4b sites, which include the three atoms in the middle of the supercell edges and the atom in the center of the supercell. The Mn and Al alternatingly occupy the remaining sites (4b and 4d),

[a)]pavel.lukashev@uni.edu
[b)]parashu.kharel@sdstate.edu

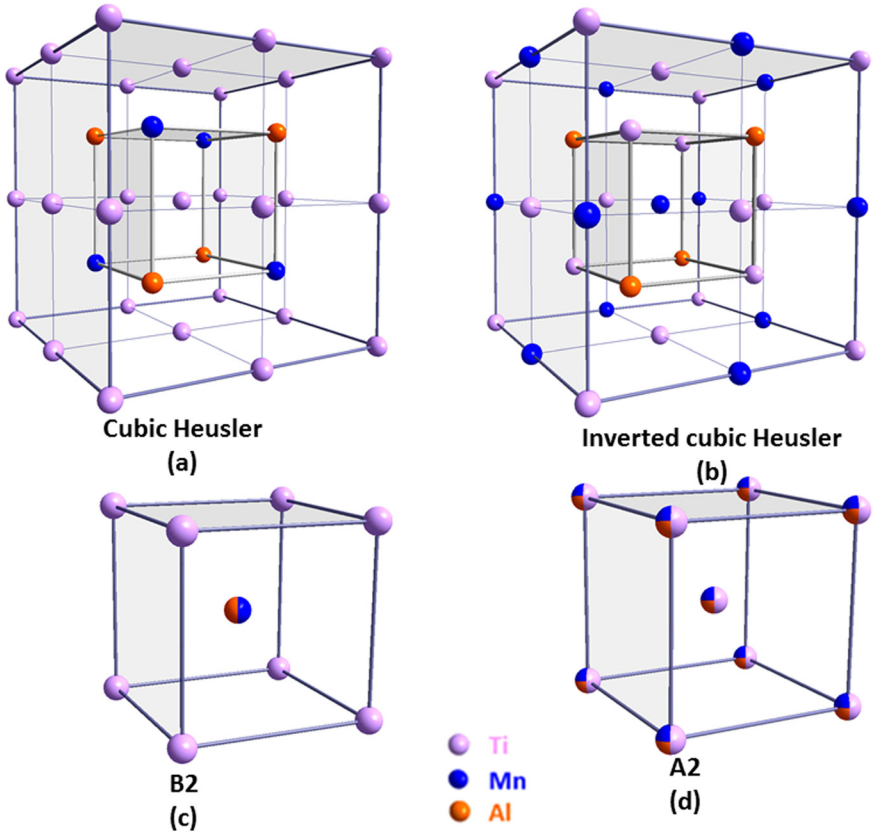

FIG. 1. Crystal structures of Ti_2MnAl and related alloys: (a) regular cubic Heusler structure, (b) inverted cubic Heusler structure, (c) disordered B2 (CsCl) structure, and (d) disordered A2 (bcc) structure.

which are all located in the middle of the bcc unit cells. In the inverted structure, the Ti 4b and Mn 4c (or 4d) atoms interchange their positions, as one can see by comparing Figs. 1(a) and 1(b). As we will see below, this inversion has far-reaching implication for electronic structure and magnetism.

The purpose of this paper is to theoretically investigate the electronic and magnetic structures of Ti_2MnAl and examine how these properties can be tuned and improved by substitutions of elements such as Sn and In for Al.

We have performed electronic-structure calculations for bulk Ti_2MnAl, $Ti_2MnAl_{0.5}In_{0.5}$, and $Ti_2MnAl_{0.5}Sn_{0.5}$, each in the regular and inverted cubic Heusler structures. We employ density-functional calculations using the projector augmented-wave method (PAW) by Blöchl,[15] implemented by Kresse and Joubert in the Vienna *ab initio* simulation package (VASP)[16] within the Perdew-Burke-Ernzerhof (PBE) generalized-gradient approximation (GGA).[17] The Methfessel-Paxton integration method[18] with a 0.05 eV width of smearing is used, along with plane-wave cut-off energy of 500 eV and convergence criteria of 10^{-3} meV for the total energy calculations. A $12 \times 12 \times 12$ k-point mesh is used for the Brillouin-zone integration. Some of the results are obtained using the MedeA® software environment.[19] All calculations are performed for the

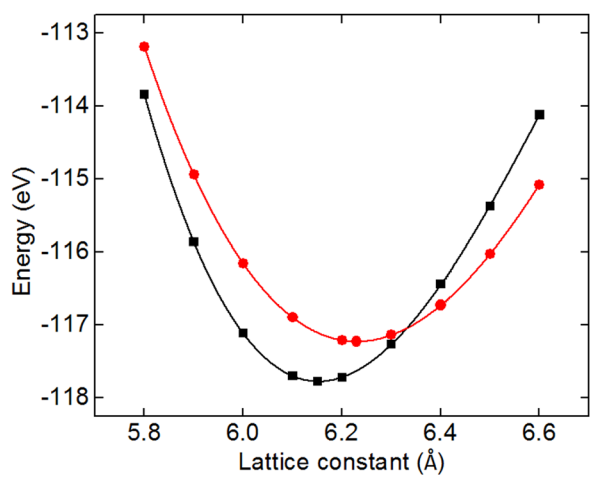

FIG. 2. Total energy per supercell of Ti_2MnAl as a function of lattice parameter. Black squares and red circles denote the regular and inverted cubic Heusler structures, respectively.

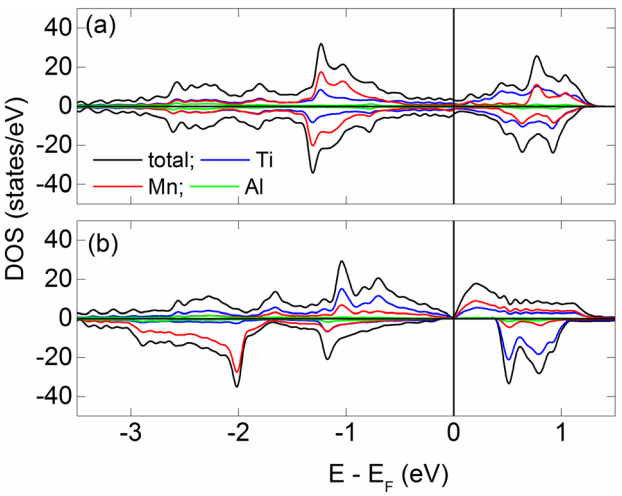

FIG. 3. Total and local DOS in Ti_2MnAl: (a) regular cubic Heusler structure and (b) inverted cubic Heusler structure. The vertical line indicates the Fermi level, and the lattice constants of 6.15 Å (a) and 6.23 Å (b) correspond to the minimum energies in Fig. 2.

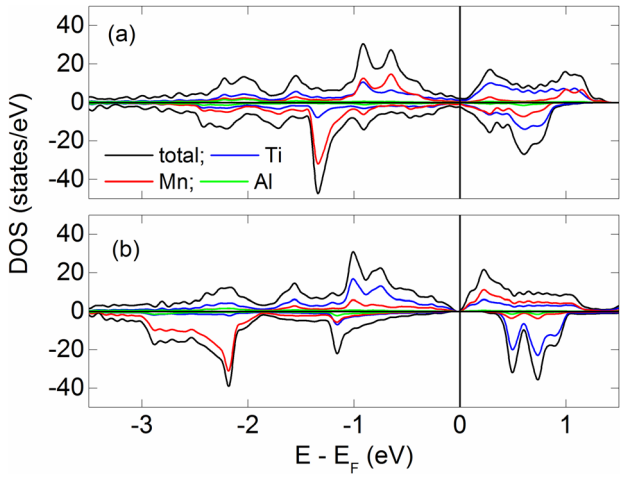

FIG. 4. Total and local DOS in Ti_2MnAl: (a) regular cubic Heusler structure and (b) inverted cubic Heusler structure. The vertical line indicates the Fermi level, and the lattice constant is taken as 6.40 Å in both (a) and (b).

16-atom cubic supercell shown in Figs. 1(a) and 1(b), with periodic boundary conditions.

Figure 2 plots the calculated energies E per 16-atom supercell as a function of the lattice parameter a for both the regular and inverted cubic Heusler phases of Ti_2MnAl. The calculated equilibrium lattice constants for the regular and inverted structures are 6.15 Å and 6.23 Å, respectively. The ground-state structure, defined as the structure of lowest energy, is the regular structure. However, at $a = 6.33$ Å, a phase transition occurs, and for larger lattice constants, the inverted structure is energetically more favorable than the regular one. The transition occurs at a tensile strain of less than 3%, a significant but experimentally attainable value, for example, in a thin-film geometry. Our calculated lattice parameters (including possible phase transition at tensile strain) are consistent with previous predictions.[3]

Figure 3 shows the calculated DOS in Ti_2MnAl for both regular and inverted structures at the optimal lattice constants. The regular ground-state phase (a) is metallic, whereas the inverted phase (b) exhibits an SGS DOS, that is, a wide band gap for the minority and a zero band gap for the majority spin channels. We have also analyzed the DOS of Ti_2MnAl at $a = 6.40$ Å, slightly above the transition lattice parameter of 6.33 Å. The results are summarized in Fig. 4, from which we see that the regular phase (a) remains metallic whereas the inverted phase (b) retains its SGS behavior. In other words, a tensile strain of about 3% causes Ti_2MnAl to undergo a phase transition from a regular metallic phase to an inverted cubic SGS phase. The band gap, 0.4 eV, is consistent with the value reported in Ref. 3.

TABLE I. Calculated magnetic moments in Ti_2MnAl at minimum-energy and fixed (6.40 Å) lattice parameters. The Ti-1 and Ti-2 sites are explained in the Introduction.

Lattice constant (Å)	Type	Ti-1 μ_B/atom	Ti-2 μ_B/atom	Mn μ_B/atom	Al μ_B/atom	Total μ_B/supercell
6.15	Regular	0.072	0.072	−0.209	0.000	−0.281
6.23	Inverted	1.385	1.216	−2.533	0.002	0.000
6.40	Regular	0.504	0.504	−1.133	0.006	−0.245
6.40	Inverted	1.512	1.363	−2.883	−0.001	0.000

The transition from metallic to SGS behavior in Ti_2MnAl is, in part, caused by the change in the crystal field due to the decreased hybridization between Ti and Mn states. As one can see from Figs. 3 and 4, the minority spin states of Ti and Mn have comparable contributions to the conduction band in the regular phase, whereas in the inverted phase, the empty minority spin states above the Fermi level are almost entirely from Ti, a clear indication of reduced Ti-Mn hybridization.

Table I summarizes the calculated magnetic moments of Ti_2MnAl for both regular and inverted structures. For the equilibrium lattice parameters, the regular phase is essentially non-magnetic, as the atomic moments of all the constituent elements are nearly zero. Note that the sum of all atomic moments slightly deviates from the total moment (by about $0.02\mu_B$ per atom) because the local charge and magnetization are calculated in atomic spheres which do not exactly fill the entire space of the unit cell.

The inverted phase is a fully compensated ferrimagnet, that is, the total magnetic moment is zero due to the cancellation of antiparallel Ti and Mn moments. This result is also in good agreement with the previously published computational report.[3] However, at larger lattice parameters, for example, at $a = 6.40$ Å, both phases behave similarly, like almost fully compensated ferrimagnets (see rows 4 and 5 in Table I). The creation of pronounced local moments in expanded regular Ti_2MnAl is probably due to the larger interatomic distances between Mn and Ti, which lead to a reduction of the Mn-Ti hybridization.[3]

As discussed above, tensile strain of about 3% is predicted to turn Ti_2MnAl into a spin gapless semiconductor. This suggests a strategy to design Ti_2MnAl-based SGS or HM compounds in which the lattice parameters can be tuned by

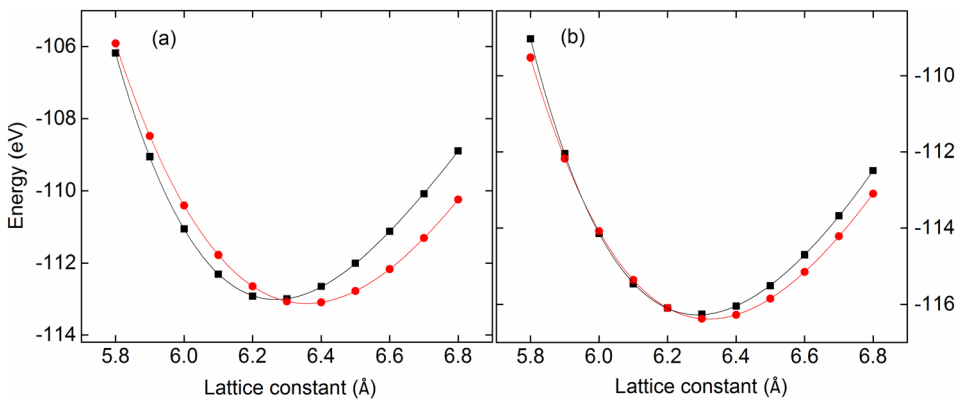

FIG. 5. Total energy per supercell as a function of lattice parameter: (a) $Ti_2MnAl_{0.5}In_{0.5}$ and (b) $Ti_2MnAl_{0.5}Sn_{0.5}$. Black squares and red circles denote the regular and inverted cubic Heusler structures, respectively.

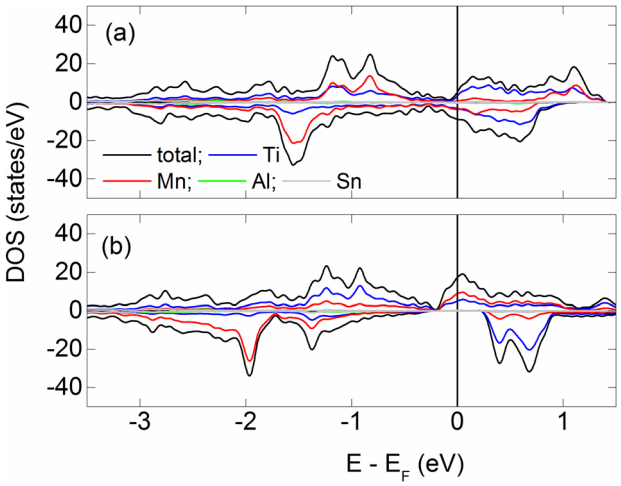

FIG. 6. Total and local DOS in $Ti_2MnAl_{0.5}Sn_{0.5}$: (a) regular cubic Heusler structure and (b) inverted cubic Heusler structure. The vertical line indicates the Fermi level, and the lattice constants of 6.289 Å (a) and 6.311 Å (b) correspond to the minimum energies of Fig. 5(b).

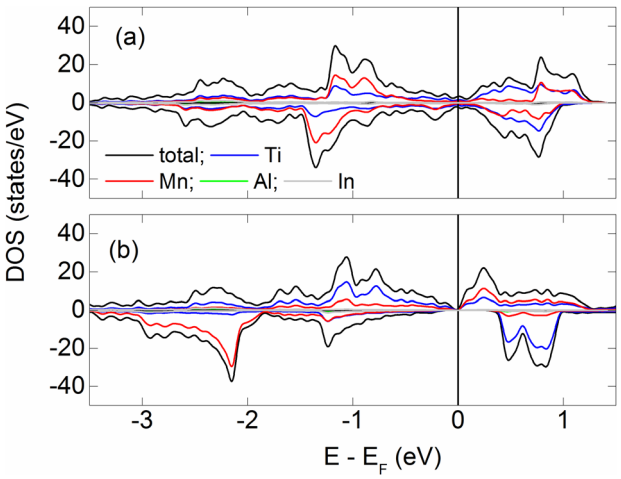

FIG. 7. Total and local DOS in $Ti_2MnAl_{0.5}In_{0.5}$: (a) regular cubic Heusler structure and (b) inverted cubic Heusler structure. The vertical line indicates the Fermi level, and the lattice constants of 6.267 Å (a) and 6.357 Å (b) correspond to the minimum energies of Fig. 5(b).

elemental substitutions. Based on this materials-by-design strategy, we have performed a series of calculations for Ti_2MnAl where 50% of the Al atoms are replaced by elements having larger atomic radii, such as Si, Ga, Ge, In, and Sn. Partial substitution of In and Sn for Al, yielding $Ti_2MnAl_{0.5}In_{0.5}$ and $Ti_2MnAl_{0.5}Sn_{0.5}$, produces the envisaged transition effect, whereas partial substitution of Si, Ga, and Ge for Al does not yield a SGS or HM ground-state transition. Figure 5 shows the calculated energies for $Ti_2MnAl_{0.5}In_{0.5}$ and $Ti_2MnAl_{0.5}Sn_{0.5}$, respectively. In $Ti_2MnAl_{0.5}In_{0.5}$, the minimum energies are −113.016 eV and −113.126 eV for the regular and inverted structure, realized at lattice parameters of 6.267 Å and 6.357 Å, respectively. Below $a = 6.280$ Å, the regular structure is more stable; above this value, the inverted one becomes more stable. In $Ti_2MnAl_{0.5}Sn_{0.5}$, the respective values are −116.272 eV and −116.386 eV at lattice parameters of 6.289 Å and 6.321 Å, and the transition occurs at about 6.20 Å. In both cases, the *inverted* cubic Heusler structure is therefore the ground state although the energy difference between the regular and inverted phases is rather small, about 0.1 eV per 16-atom cell.

Figures 6 and 7 elucidate the electronic structure of $Ti_2MnAl_{0.5}In_{0.5}$ and $Ti_2MnAl_{0.5}Sn_{0.5}$. Figure 6 shows the DOS of $Ti_2MnAl_{0.5}Sn_{0.5}$ in regular and inverted structures. The inverted ground state of $Ti_2MnAl_{0.5}Sn_{0.5}$ exhibits half-metallic behavior, with metallic behavior of the majority and insulating behavior of the minority electrons. By contrast, the regular phase of $Ti_2MnAl_{0.5}Sn_{0.5}$ is a spin-polarized metal. Since the inverted phase of $Ti_2MnAl_{0.5}Sn_{0.5}$ corresponds to the ground state structure, this material is a *half-metal* at ambient pressure. In the case of $Ti_2MnAl_{0.5}In_{0.5}$, Fig. 7, the regular phase is a Pauli-paramagnetic metal and the inverted phase, which corresponds to the ground-state structure, is a SGS.

Table II shows the calculated magnetic moments of $Ti_2MnAl_{0.5}Sn_{0.5}$ and $Ti_2MnAl_{0.5}In_{0.5}$ at their optimal lattice constants. The Mn atoms in $Ti_2MnAl_{0.5}Sn_{0.5}$ and $Ti_2MnAl_{0.5}In_{0.5}$ have two different values of the magnetic moment, as contrasted to in Ti_2MnAl, where all Mn atoms have the same magnetic moment by symmetry. Replacing each second Al atom by Sn or In breaks this symmetry and leads to the different Mn moments. It is worthwhile noting that the ground state of $Ti_2MnAl_{0.5}In_{0.5}$ remains a fully compensated ferrimagnet due to the antiparallel orientation of Ti and Mn moments, whereas the ground state of $Ti_2MnAl_{0.5}Sn_{0.5}$ is ferrimagnetic with a total magnetic moment of $2\mu_B$ per supercell. The non-zero total moment in $Ti_2MnAl_{0.5}Sn_{0.5}$ reflects the valence difference between Sn and In, which affects the Mn moments. Note that the integer values of the calculated total ground-state magnetic moments in $Ti_2MnAl_{0.5}In_{0.5}$ and $Ti_2MnAl_{0.5}Sn_{0.5}$ are consistent with our results that these materials are SGS and HM, respectively.

In summary, we have investigated a previously unconsidered class of materials-by-design, namely, substituted Ti_2MnAl. Our first-principles calculations indicate that $Ti_2MnAl_{0.5}Sn_{0.5}$ and $Ti_2MnAl_{0.5}In_{0.5}$ are half-metallic and spin-gapless semiconducting, respectively. In contrast to the metallic Ti_2MnAl parent compound, which has a regular cubic Heusler structure, the substituted alloys are predicted

TABLE II. Calculated magnetic moments in $Ti_2MnAl_{0.5}M_{0.5}$ at minimum-energy lattice parameters. The Ti-1 and Ti-2 sites are explained in the Introduction.

a (Å)	M	Type	Ti-1 μ_B/atom	Ti-2 μ_B/atom	Mn-1 μ_B/atom	Mn-2 μ_B/atom	Al μ_B/atom	M μ_B/atom	Total μ_B/supercell
6.289	Sn	Regular	0.394	0.394	−1.149	−1.400	0.056	0.026	−1.563
6.321	Sn	Inverted	1.510	1.253	−2.375	−2.374	0.095	0.101	2.000
6.267	In	Regular	0.215	0.215	−0.571	−0.693	0.023	0.034	−0.482
6.357	In	Inverted	1.467	1.329	−2.895	−2.895	0.080	0.102	0.000

to crystallize in the inverted cubic Heusler structure. We envision experimental research on these intriguing systems as a subject of future work.

This research is supported by Scholarly Excellence Funds and Research Support Funds, South Dakota State University. The research at University of Northern Iowa (UNI) is supported by the Pre-Tenure Grant from the Office of the Provost and Executive Vice President for Academic Affairs, UNI, as well as from the UNI Faculty Summer Fellowship. Computations were performed at the Department of Physics computing facilities, UNI. The research at University of Nebraska is supported by the U.S. department of Energy, Office of Basic Energy Sciences under Award No. DOE/BES (DE-FG02-04ER46152), and the work at Nebraska was performed, in part, in the Nebraska Nanoscale Facility, Nebraska Center for Materials and Nanoscience, which is supported by the National Science Foundation under Award No. NNCI: 1542182, and the Nebraska Research Initiative. K. Yang would like to thank the Program for Outstanding Innovative Talents in Hohai University, China.

[1]X. L. Wang, Phys. Rev. Lett. **100**, 156404 (2008).
[2]K. Özdoğan, E. Şaşioğlu, and I. Galanakis, J. Appl. Phys. **113**, 193903 (2013).
[3]H. Y. Jia, X. F. Dai, L. Y. Wang, R. Liu, X. T. Wang, P. P. Li, Y. T. Cui, and G. D. Liu, AIP Adv. **4**, 047113 (2014).
[4]P. Kharel, W. Zhang, R. Skomski, S. Valloppilly, Y. Huh, R. Fuglsby, S. Gilbert, and D. J. Sellmyer, J. Phys. D: Appl. Phys. **48**, 245002 (2015).
[5]S. Ouardi, G. H. Fecher, and C. Felser, Phys. Rev. Lett. **110**, 100401 (2013).
[6]A. Nelson, P. Kharel, Y. Huh, R. Fuglsby, J. Guenther, W. Zhang, B. Staten, P. Lukashev, S. Valloppilly, and D. J. Sellmyer, J. Appl. Phys. **117**, 153906 (2015).
[7]H. Ohno, Nat. Mater. **9**, 952 (2010).
[8]R. P. Panguluri, P. Kharel, C. Sudakar, R. Naik, R. Suryanarayan, V. M. Naik, A. G. Petukhov, B. Nadgorny, and G. Lawes, Phys. Rev. B **79**, 165208 (2009).
[9]I. M. Tsidilkovski, *Electron Spectrum of Gapless Semiconductors*, Spinger Series in Solid-State Sciences Vol. 116, edited by K. von Klitzing (Springer, New York, 1996).
[10]A. H. Castro Neto, F. Guinea, N. M. R. Peres, K. S. Novoselov, and A. K. Geim, Rev. Mod. Phys. **81**, 109 (2009).
[11]M. E. Jamer, B. A. Assaf, T. Devakul, and D. Heiman, Appl. Phys. Lett. **103**, 142403 (2013).
[12]G. Y. Guo and K. Yao, Appl. Phys. Lett. **103**, 232409 (2013).
[13]S. Skaftouros, K. Özdoğan, E. Şaşioğlu, and I. Galanakis, Appl. Phys. Lett. **102**, 022402 (2013).
[14]Q. Fang, X. Zhao, J. Zhang, and K. Xu, Thin Solid Films **558**, 241 (2014).
[15]P. Blöchl, Phys. Rev. B **50**, 17953 (1994).
[16]G. Kresse and D. Joubert, Phys. Rev. B **59**, 1758 (1999).
[17]J. P. Perdew, K. Burke, and M. Ernzerhof, Phys. Rev. Lett. **77**, 3865 (1996).
[18]M. Methfessel and A. T. Paxton, Phys. Rev. B **40**, 3616 (1989).
[19]MedeA® Version 2.16. MedeA® is a registered trademark of Materials Design, Inc. Angel Fire, New Mexico, USA.